

# Rhythmogenic effects of weak electrotonic coupling in neuronal models

(gap junctions/bursting oscillations/coupled oscillators)

ARTHUR SHERMAN AND JOHN RINZEL

National Institutes of Health, National Institute of Diabetes and Digestive and Kidney Diseases, Mathematical Research Branch, Building 31, Room 4B-54, Bethesda, MD 20892

Communicated by William A. Hagins, December 20, 1991

**ABSTRACT** Strong gap-junctional coupling can synchronize the electrical oscillations of cells, but we show, in a theoretical model, that weak coupling can phase lock two cells 180° out-of-phase. Antiphase oscillations can exist in parameter regimes where in-phase oscillations break down. Some consequences are (i) coupling two excitable cells leads to pacemaking, (ii) coupling two pacemaker cells leads to bursting, and (iii) coupling two bursters increases burst period. The latter shows that details of the fast spikes can affect macroscopic properties of the slow bursts. These effects hold in other models for bursting and may play a role in the collective behavior of cellular ensembles.

Strong gap-junctional coupling is well-suited for imposing synchronization on electrically active cells such as neurons or heart pacemaker cells. Here we demonstrate that weak coupling can lead to qualitative changes in electrical activity and can dramatically expand the repertoire of available behaviors. The core phenomenon is the emergence of action potentials that are 180° out-of-phase (or antiphase) when two oscillatory, or excitable nonoscillatory, cells are weakly coupled. In the context of bursting oscillations, the development of antiphase oscillations on the microscale of spike activity has consequences for the macroscale of the bursts; weak coupling can significantly increase burst period and bursting can be induced in tonically spiking cells.

## THEORETICAL MODEL

We illustrate with a model that is representative of a class of models called “square-wave bursters” (1). The model used here is a simplified version of a biophysically based model for bursting in pancreatic  $\beta$  cells (2). Other examples include a model for thalamic neurons (3) and another based on a model for barnacle muscle fibers (4). A typical square burster time course is shown in Fig. 3A.

The equations are

$$\tau \frac{dV}{dt} = -I_{in}(V) - I_{out}(V, n) - g_s S(V - V_K) + I \quad [1]$$

$$\tau \frac{dn}{dt} = \lambda(n_\infty - n). \quad [2]$$

Eq. 1 is the current balance equation for the membrane potential  $V$ . The  $V$ -dependent ionic currents include a fast inward ( $\text{Na}^+$  or  $\text{Ca}^{2+}$ ) current and an outward (delayed rectifier  $\text{K}^+$ ) current with its fractional activation,  $n$ , varying on a 20-ms time scale. The  $g_s$  term in Eq. 1 is a slow outward current that varies on a time scale of seconds. For example,

$S$  could be intracellular  $\text{Ca}^{2+}$  that slowly accumulates and activates a  $\text{K}^+$  current (2), a voltage-independent ATP-blockable  $\text{K}^+$  conductance (5), or a slow inactivation component of  $\text{Ca}^{2+}$  current (6). For neurons, another possibility is recurrent inhibition onto a slow synapse. Initially, we consider  $S$  to be constant, but later, to produce bursting, we make  $S$  a slow variable by adding feedback dynamics. Gap-junction coupling is represented by adding one more term to Eq. 1 that represents junctional current:  $I_j = -g_c(V - \bar{V})$ , where  $\bar{V}$  is the membrane potential of the neighboring cell.

Solutions for Figs. 1 and 2 were computed on an IBM PS/2 model 80 with the program PHASEPLANE (7), a commercial package for numerical integration and analysis that requires a minimum of programming. The integration method was set to the Gear algorithm (8) with an error tolerance of  $10^{-7}$ . For the bursting solutions of Figs. 3 and 4, it was convenient to use a FORTRAN-callable Gear solver on a faster machine, an IBM AIX/370 mainframe. All calculations were carried out in double precision.

## RESULTS

We demonstrate first the basic phenomenon of antiphase spiking by considering nonbursting cells (i.e., we hold  $S$  fixed in Eq. 1). For  $S = 0.15$ , an isolated model cell is a spontaneously spiking pacemaker. If two such identical oscillating cells are coupled electrically and are precisely in-phase, no current will flow between them. Their time courses will remain in-phase and will satisfy the single cell equations. If the coupling is weak, however, this in-phase solution may be unstable and the slightest perturbation will destroy the synchrony, leading to a new spike pattern with the cells 180° out-of-phase (Fig. 1).

The antiphase action potentials are of smaller amplitude because each cell receives hyperpolarizing input at its peak and depolarizing input at its minimum. The minimum is affected more than the maximum since  $g_c$  is larger compared to the other conductances when the membrane potential is more negative. The reduction in amplitude is accompanied by a reduction in period (from  $\approx 190$  to 120 ms) primarily because the spikes are initiated from a depolarized level where the time constant is smaller.

The process is reversible; if coupling is removed the cells will revert to their individual oscillation (although they will be out-of-phase). Alternatively, increasing  $g_c$  sufficiently will destabilize the antiphase solution, restabilize the single-cell solution, and synchronize the cells. (Fig. 1, right arrow). (Smaller increases in  $g_c$  can lead to other complex behavior that is neither phase locked nor periodic.) Desynchronization is necessarily a slow process because  $g_c$  is small; for very weak coupling, the approach to the antiphase oscillation is exponential with a time constant that varies inversely with  $g_c$ . In the case of Fig. 1,  $\approx 20$  spikes are needed to converge to

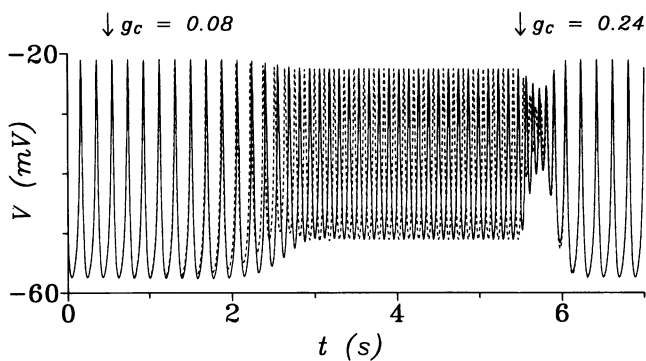


FIG. 1. Weakly coupled cells can oscillate antiphase. Solution of Eqs. 1 and 2 with  $S = 0.15$  and  $\lambda = 0.8$ . Two cells, initially uncoupled, are started at identical phases. Membrane potential versus time for one cell is shown solid, and for the other is dashed. At  $t = 0.5$  s the junctional-coupling conductance,  $g_c$ , is raised to 0.08, and a small symmetry-breaking perturbation (0.3 mV) is applied to one of the cells. This destabilizes the single-cell oscillation and leads to an antiphase oscillation. At  $t = 5.5$  s the single-cell behavior is restored by increasing  $g_c$  to 0.24; alternatively, one could set  $g_c$  to 0, but then the two cells would not be in-phase. In Eq. 1,  $I_{in}(V) = g_{Ca}m(V - V_{Ca})$ ,  $I_{out}(V) = g_Kn(V - V_K)$ .  $m$  is assumed to be fast so  $m = m_{\infty}(V)$ , while  $n$  satisfies Eq. 2.  $x_{\infty}(V) = 1/[1 + \exp((V_x - V)/\theta_x)]$ ;  $x = m, n$ . Parameters (mV):  $V_m = -20$ ,  $\theta_m = 12$ ,  $V_n = -17$ ,  $\theta_n = 5.6$ ,  $V_{Ca} = 25$ ,  $V_K = -75$ . The effective time constant,  $\tau$ , for Eq. 1 is 20 ms; the time constant for Eq. 2 is  $\tau/\lambda$ ,  $\lambda = 0.8$  or  $0.9$  as noted. The maximal conductances  $g_{Ca} = 3.6$ ,  $g_K = 10$ , and  $g_s = 4$  have been scaled by a typical instantaneous conductance in order to define  $\tau$  and so are dimensionless; values of coupling conductance,  $g_c$ , in the text are then relative to a typical conductance.  $I$  is the nondimensional applied current (Fig. 2 only).

the antiphase solution. Resynchronization is much faster because  $g_c$  has been increased by a factor of 3.

If an isolated cell is hyperpolarized by fixing  $S$  at a large enough value, it is no longer self-oscillatory, but it remains excitable. When a stimulating current is applied, the cell fires repetitively; firing ceases once the stimulus is withdrawn (Fig. 2). After two identical such cells are coupled and the stimulus to one cell is repeated, the cells enter an antiphase

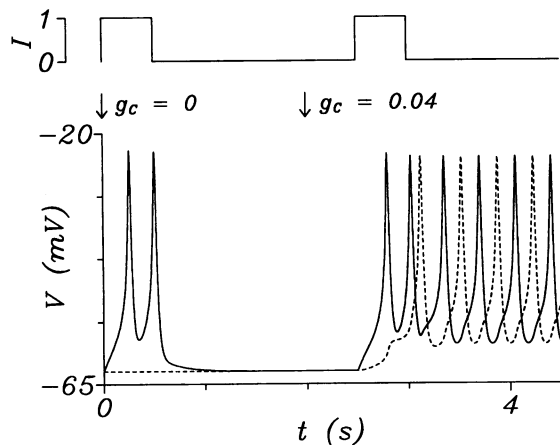


FIG. 2. Weak coupling can convert excitable cells into spikers. The cells are the same as in Fig. 1, but with  $S = 0.177$ . Again, membrane potential time course for one cell is solid, and for the other is dashed. Cells are initially uncoupled and at rest, but one cell (solid line) has a current of strength 1.0 injected for 0.5 s, resulting in two spikes. Spiking ends when the current stimulus is removed. The unstimulated cell (dashed line) remains at rest. At  $t = 2$  s,  $g_c$  is increased to 0.04. This does not prevent the stimulated cell from remaining at rest, but the system is now bistable and the rest state coexists with an antiphase oscillation. A second identical current stimulus draws both cells near enough to the oscillatory solution so that they continue to oscillate after the stimulus terminates.

oscillation that persists indefinitely after the applied current is removed. Unlike the first example (Fig. 1), where coupling converted one type of oscillation (in-phase) into another (antiphase), now coupling allows spiking where an unstimulated, isolated cell cannot oscillate at all. Coupling has extended the range of  $S$  values for which oscillations exist by making the cells bistable: they can sit at a fixed voltage or oscillate antiphase. The second stimulus raises the cells above threshold for antiphase spiking. (Current could be applied to both cells, but without, say, 10% asymmetry there may be insufficient time to go antiphase before falling below threshold.) The pair of cells can be reset to rest by increasing or eliminating  $g_c$ , or, because of bistability, by a hyperpolarizing or depolarizing current.

Next we consider cells with endogenous bursting properties. Now  $S$  is a slow dynamic variable, satisfying

$$\tau_s \frac{dS}{dt} = S_{\infty}(V) - S, \quad [3]$$

with  $\tau_s \gg \tau$ , and the model has three variables. In models in which  $S$  represents free intracellular  $Ca^{2+}$ , the  $S$  equation is a  $Ca^{2+}$ -balance equation (2). In general, Eq. 3 has the property that  $S$  slowly increases when the cell is depolarized and slowly decreases when the cell is hyperpolarized. With  $\lambda = 0.9$ , an isolated cell alternates periodically between a depolarized spiking phase and a hyperpolarized silent phase (Fig. 3A). This square wave burst pattern reflects bistability of the spike-generating subsystem. Over the range of values swept (up and down) by  $S$  in one period, Eqs. 1 and 2 have two coexistent stable modes of behavior: a depolarized state of repetitive spiking and a steady "resting" state of hyperpolarization.

When two identical bursters are coupled with  $g_c = 0.06$  and started in-phase, they initially follow the single-cell bursting solution (Fig. 3B). This behavior is unstable, however, and a new stable burst pattern emerges during the second burst with smaller amplitude, higher frequency, antiphase spikes (Fig. 3C). The amplitude of  $S$ , and consequently the burst period, are substantially increased. As shown in Fig. 2, coupling has extended the range of  $S$  over which the cells are bistable and oscillatory by creating a new depolarized state of antiphase spiking. As for the cases shown in Figs. 1 and 2, reducing  $g_c$  to 0 or raising it sufficiently restores the single-cell behavior.

If  $\lambda$  is made very large ( $\approx 10$ ), Eqs. 1 and 2 are no longer oscillatory but bistable with high- and low-voltage resting states. When combined with Eq. 3, the result is not bursting but a slow wave or relaxation oscillation. When two such oscillators are weakly coupled there is no period extension as in Fig. 3; if the cells differ slightly, the period can even decrease. This is significant because one often assumes for simplicity that the fast time scale phenomena can be averaged out or ignored when studying bursting (9). While that approach is often justified, the properties of oscillators can depend on the existence of spikes as opposed to a simple plateau.

For our final example, we consider a case in which coupling converts tonic spiking cells to bursters. In an isolated cell, reducing  $\lambda$  increases the spike amplitude, and bursting may give way to large-amplitude spiking, which can be viewed as bursts with one spike (Fig. 4, left arrow). This beating solution is similar to the early spikes of Fig. 1, except there  $S$  is constant, while in Fig. 4  $S$  undergoes a small-amplitude oscillation. When two cells are coupled with  $g_c = 0.04$ , bursting is restored, and the amplitude of  $S$  is increased 8-fold. Again, the spikes are antiphase.

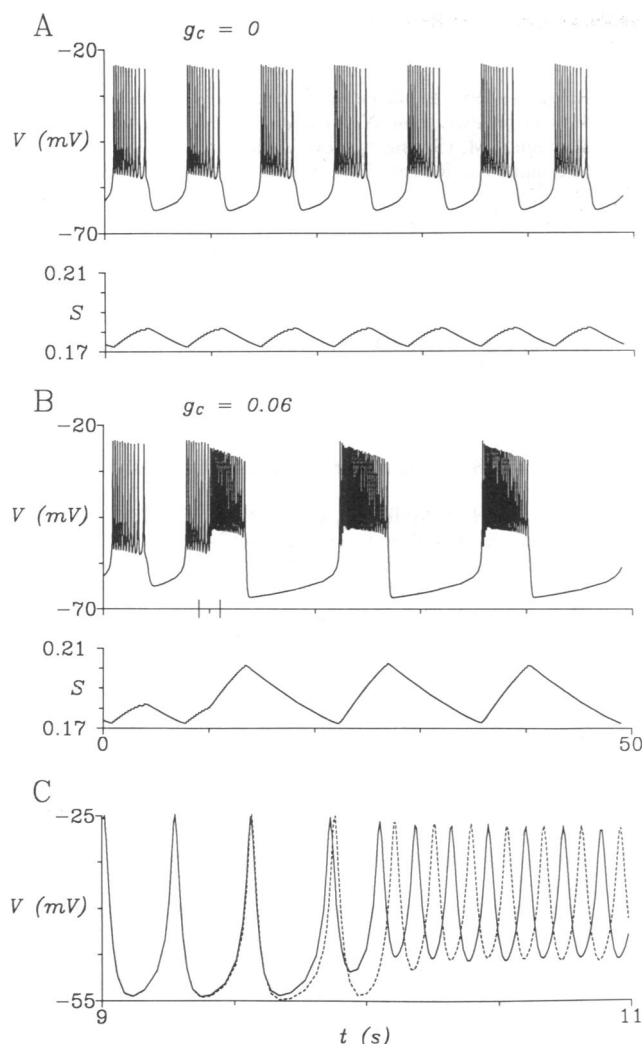


FIG. 3. Weak coupling can increase the period of bursting. (A) Solution of Eqs. 1–3 ( $V$ , Upper;  $S$ , Lower) for an uncoupled bursting cell.  $S$  is now a slow variable ( $\tau_s = 35$  s) that increases during the active phase and decreases during the silent phase. Note the long time scale compared to Figs. 1 and 2. Parameters are the same as in Figs. 1 and 2, except  $\lambda = 0.9$ , which reduces spike amplitude and makes Eqs. 1 and 2 bistable over the range of  $S$  traversed during bursting.  $S_\infty(V)$  has the form of  $x_\infty(V)$  (see Fig. 1) with  $V_s = -38$  mV and  $\theta_s = 10$  mV. (B) Two bursters (only one shown) are coupled with  $g_c = 0.06$  and started with identical initial conditions. No perturbation is applied; accumulated numerical errors are enough to destabilize the single-cell solution and lead to a new solution with the burst period doubled and  $S$  amplitude tripled. The time courses of the two cells are almost identical on the bursting time scale, but an expanded view (C) of both cells (one shown as solid line, and one shown as dashed line) during the interval corresponding to the long ticks in B shows that the spikes undergo a transition from in-phase to antiphase spiking. Antiphase spiking persists in the second and succeeding bursts (data not shown), with the lead alternating between the two cells.

## DISCUSSION

Summarizing, we see that weak gap-junctional coupling can give rise to antiphase oscillations (Fig. 1), which extend the parameter ranges for oscillatory behavior beyond those of isolated or strongly coupled cells (Figs. 2 and 3). Modulation of coupling conductance can then switch the behavior of the two cells between silent and oscillatory (Fig. 2) or between simple oscillations and bursting (Fig. 4).

The idea that electrotonic coupling can lead to antiphase oscillations is counterintuitive. Rather, one often thinks of

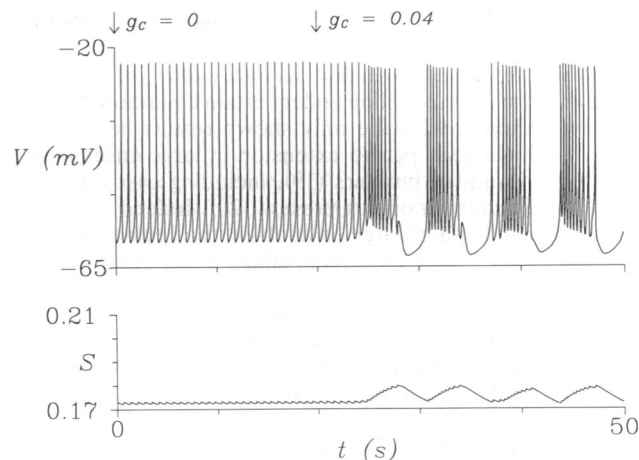


FIG. 4. Weak coupling can convert spikers to bursters. Parameters are the same as in Fig. 3, except  $\lambda = 0.8$ , resulting in repetitive spiking (beating) instead of bursting. Oscillations in  $S$  are nearly abolished. Two identical cells are started with identical initial conditions (only one shown for clarity). At  $t = 20$  s,  $g_c$  is increased to 0.04 (right arrow) and a small symmetry-breaking perturbation (0.3 mV) is applied to one cell. After a brief transient, the two cells begin to burst in-phase but with antiphase spikes, as in Fig. 3.

reciprocal activity as resulting from mutual inhibition through the mechanism of postinhibitory rebound (10, 11). Indeed, because gap-junctional current is hyperpolarizing when the neighboring cell has a more negative potential and depolarizing when the neighbor has a higher potential, one expects coupling to equalize the cells' potentials. This is the case when coupling is strong, but it need not be so when coupling is weak. One way to predict the effect of weak coupling between oscillators is to examine the average coupling current over a period (12). When the average coupling is in a certain sense "mutually inhibitory," the oscillators will tend to repel each other. Then the stable situation is for the phases to be as far apart as possible—i.e.,  $180^\circ$  apart. We carried out numerical perturbation calculations (unpublished data, but a technique described in ref. 13 was used) to verify that the averaged coupling current for our examples is such as to result in antiphase solutions.

Our intuition, and indeed our ability to find parameter values to illustrate the phenomena, is primarily based on such calculations and also our understanding of the geometry of solutions in parameter space. (For the case of an isolated cell, see ref. 14; the extension to two cells is unpublished.) Given the existence of antiphase oscillations, however, one can interpret biophysically the period extension when two bursters are coupled. In the bursting regime, the membrane is bistable with a depolarized oscillatory state and a hyperpolarized steady state separated by a threshold. During the active phase,  $S$  slowly increases, making the membrane less excitable by raising the threshold. The spike minima also hyperpolarize slightly, and the burst ends when the two meet. When the cells are coupled and spike out-of-phase, the spike minima are depolarized (Figs. 1 and 3) and are farther above the threshold, which is unaffected. Thus, a larger value of  $S$  is required to terminate the burst, and the active phase duration increases. The silent phase duration also increases since it takes longer for  $S$  to decay sufficiently to allow spiking to resume.

For several reasons, we believe that the results seen here for a particular, idealized model have a broader application. Our illustrative model uses ionic currents found ubiquitously in neurons, secretory cells, and other electrically active cells. All the square-wave burster models tested (2–4) show both antiphase oscillations and the macroscopic consequences

seen here. Moreover, examples of antiphase oscillations can be found in neuroscience (15) and chemistry (16), and mathematical analysis indicates that they are a likely consequence of weak diffusional coupling under certain conditions (17, 18). Finally, although we have only shown results here for cell pairs, we have seen period extension in large ensembles of electrically coupled bursters (19), including cases in which substantial channel noise is present (20). Indeed, since it is harder to synchronize large ensembles, the period-extension effect persists for much larger values of coupling conductance. With many deterministic cells, the spikes are not antiphase; rather, the phase relations drift in a complicated, possibly chaotic way (compare to ref. 21).

We conclude with some speculations about possible applications of the rhythmogenic phenomena discussed here to neuronal networks.

If two neurons provide synaptic input to one target cell, antiphase oscillations would yield a smoother signal than in-phase oscillations. Lewis (15) has explored antiphase spiking in an electronic motoneuron model as a way to obtain coordinated, but not perfectly synchronous, signals and thus avoid jerkiness of muscular response.

Two neurons with the properties shown in Fig. 2 could have interesting switching behavior if their gap junctions were modifiable (say, by cAMP). When the junctions were open, brief synaptic input to one cell could evoke a steady oscillatory output from the pair, but only a transient response would be possible when they were closed.

An important question is how much of the detailed biophysical properties of neurons are important for understanding neural networks, especially in view of recent interest in theoretical networks composed of very simplified units. Rather than give an answer here, we offer our examples as provocative instances where the details do make a difference in gross behavior. One may consider whether such enhancements of the collective behavior of cells have implications for information processing at the network level.

We thank G. B. Ermentrout for providing a computer code for the perturbation calculations and the National Institutes of Health Di-

vision of Computer Research and Technology for providing computer time on the AIX/370 system.

1. Rinzel, J. (1987) in *Mathematical Topics in Population Biology, Morphogenesis, and Neurosciences*, eds. Teramoto, E. & Yamaguti, M. (Springer, New York), pp. 267–281.
2. Sherman, A., Rinzel, J. & Keizer, J. (1988) *Biophys. J.* **54**, 411–425.
3. Hindmarsh, J. & Rose, M. (1984) *Proc. R. Soc. London B* **221**, 87–102.
4. Morris, C. & Lecar, H. (1981) *Biophys. J.* **35**, 193–213.
5. Keizer, J. & Magnus, G. (1989) *Biophys. J.* **56**, 229–242.
6. Satin, L. & Cook, D. (1989) *Pflügers Arch.* **414**, 1–10.
7. Ermentrout, B. (1990) *PHASEPLANE* (Brooks/Cole, Pacific Grove), Version 3.0.
8. Gear, C. W. (1971) *Numerical Initial Value Problems in Ordinary Differential Equations* (Prentice-Hall, Englewood Cliffs, NJ).
9. Kepler, T. B., Marder, E. & Abbott, L. F. (1990) *Science* **248**, 83–85.
10. Perkel, D. H. & Mulloney, B. (1974) *Science* **185**, 181–183.
11. Satterlie, R. A. (1985) *Science* **229**, 402–404.
12. Kopell, N. (1988) in *Neural Control of Rhythmic Movements in Vertebrates*, eds. Cohen, A. H., Rossignol, S. & Grillner, S. (Wiley, New York), pp. 369–414.
13. Ermentrout, G. B. & Kopell, N. (1991) *J. Math. Biol.* **29**, 195–217.
14. Rinzel, J. (1985) in *Ordinary and Partial Differential Equations*, eds. Sleeman, B. D. & Jarvis, R. J. (Springer, New York), pp. 304–316.
15. Lewis, E. R. (1968) in *Cybernetic Problems in Bionics*, ed. Oestreich, H. L. (Gordon & Breach, New York), pp. 777–789.
16. Crowley, M. F. & Epstein, I. R. (1989) *J. Phys. Chem.* **93**, 2496–2502.
17. Kawato, M., Sokabe, M. & Suzuki, R. (1979) *Biol. Cybernet.* **34**, 81–89.
18. Aronson, D. G., Ermentrout, G. B. & Kopell, N. (1990) *Physica D* **41**, 403–449.
19. Rinzel, J., Sherman, A. & Stokes, C. L. (1992) in *Analysis and Modeling of Neural Systems*, ed. Eeckman, F. (Kluwer, New York), pp. 29–46.
20. Sherman, A. & Rinzel, J. (1991) *Biophys. J.* **59**, 547–559.
21. Kuramoto, Y. (1978) *Prog. Theor. Phys. Suppl.* **64**, 346–367.